Science Advances
AAAS

Supplementary Materials for

Amilorides inhibit SARS-CoV-2 replication in vitro by targeting RNA structures

Martina Zafferani, Christina Haddad, Le Luo, Jesse Davila-Calderon, Liang-Yuan Chiu, Christian Shema Mugisha, Adeline G. Monaghan, Andrew A. Kennedy, Joseph D. Yesselman, Robert J. Gifford, Andrew W. Tai, Sebla B. Kutluay, Mei-Ling Li*, Gary Brewer*, Blanton S. Tolbert*, Amanda E. Hargrove*

*Corresponding author. Email: lime@rwjms.rutgers.edu; brewerga@rwjms.rutgers.edu; bst18@case.edu; amanda.hargrove@duke.edu

Published 26 November 2021, *Sci. Adv.* **7**, eabl6096 (2021)
DOI: 10.1126/sciadv.abl6096

This PDF file includes:

Supplementary Text

I. Small Molecule screening against OC43 with Vero E6 cells

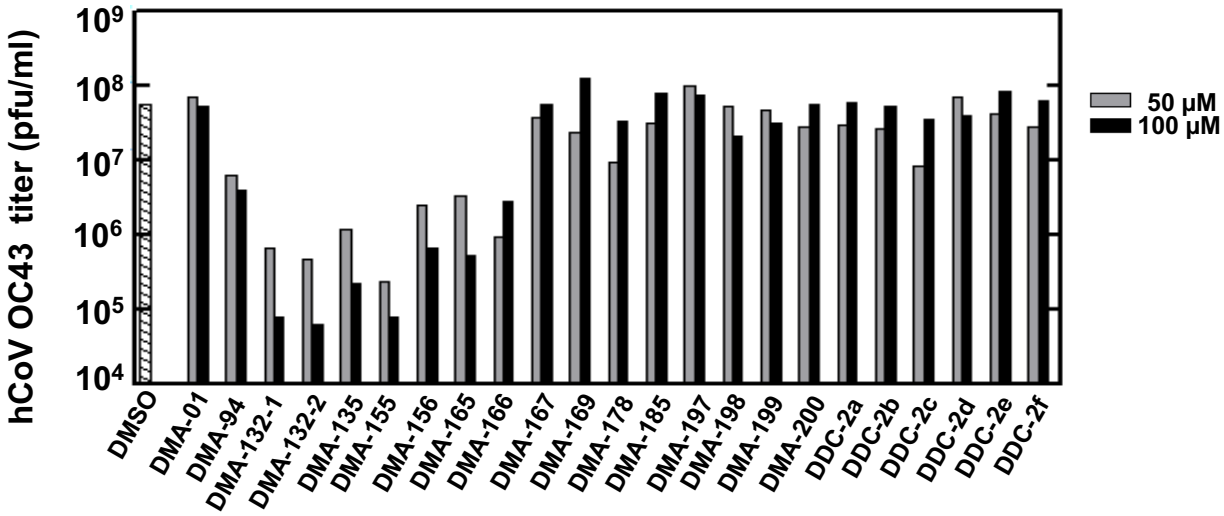

Figure S1. **Vero E6 cells were infected with human coronavirus OC43 at an MOI 1**. Various concentrations of DMAs were added to the cells. Media were harvested 24 hr post-infection and assayed for infectious virus by plaque formation with Vero E6 cells.

II. Replicates of antiviral effects of lead DMAs

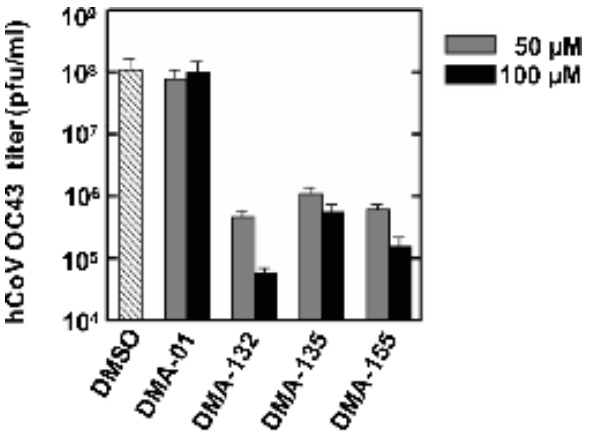

Figure S2. **Vero E6 cells were infected with human coronavirus OC43 at an MOI 1.** DMAs were added to the cells at 50 µM or 100 µM. Media were harvested 24 hr post-infection and assayed for infectious virus by plaque formation with Vero E6 cells. Mean values and standard deviations from three independent experiments are shown in the bar graphs. $P < 0.01$ for all three DMAs.

III. Small molecule toxicity in Vero E6 cells

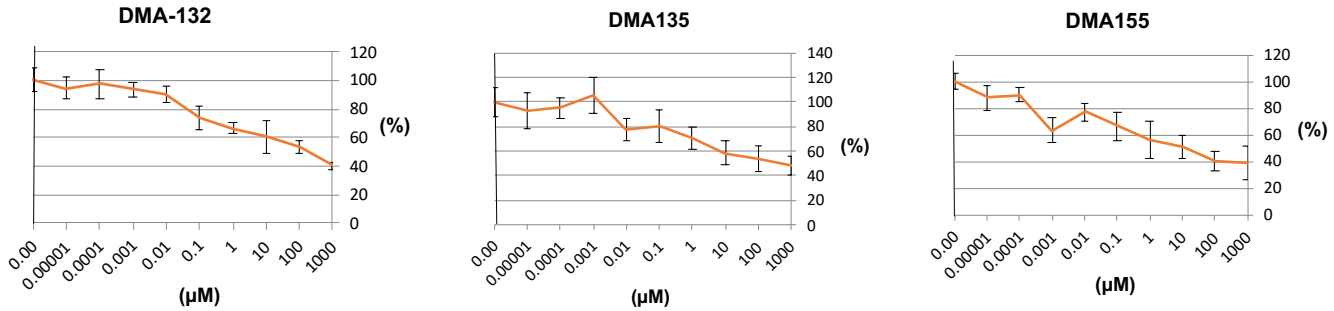

Figure S3. **Cytotoxicity assay shows the CC_{50} of DMA-132 and -135 in Vero E6 cells were > 100 µM. CC_{50} of DMA-155 was about 90 µM**. Various concentrations of DMAs were added to Vero E6 cells. Cells were incubated at 33°C for 96 hrs. Cell viability was determined by MTT assay with measurements at 570 nm according to the manufacturer's instructions (EMD Millipore). All experiments were performed in triplicate.

IV. Q-RT-PCR assay for dose dependent antiviral activity

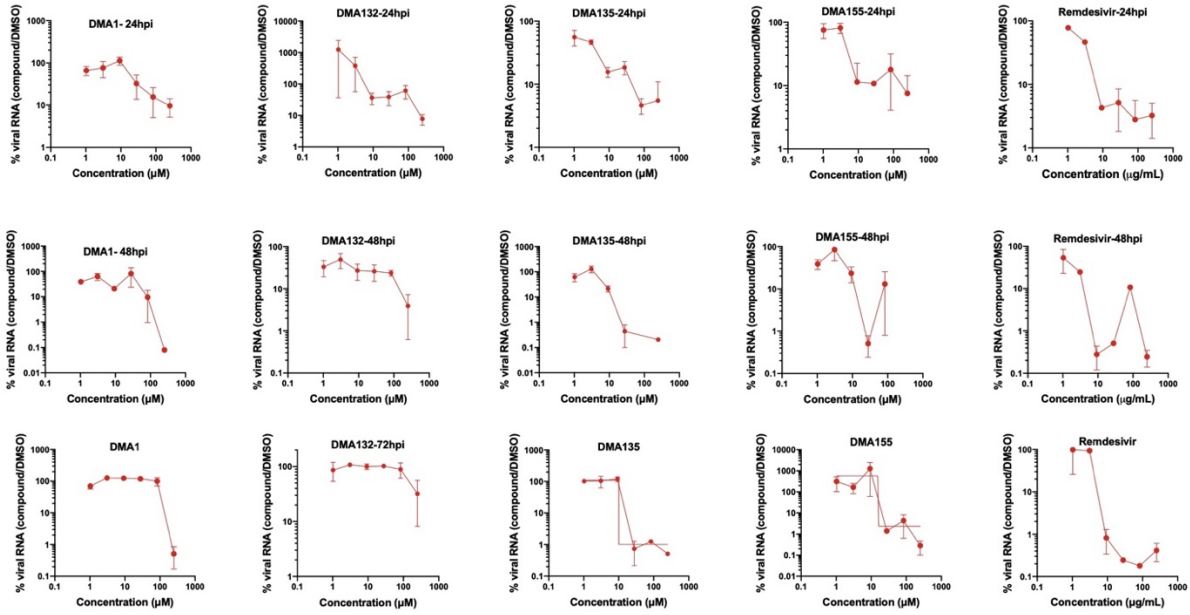

Figure S4. **qRT-PCR assay of DMA leads in SARS-CoV-2 infected cells.** Vero E6 cells were infected with SARS-CoV-2 at MOI: 0.1 i.u./cell and the indicated DMA compounds were added on cells following virus adsorption for 1 hr. Cell culture supernatants were collected and analyzed by a Q-RT-PCR assay using N-specific primers. Data show the relative percentage of viral RNA in DMA-treated samples compared to mock-treated samples at 24, 48, and 72 hours. Data are from two independent experiments and error bars show the range.

V. ^{13}C -HSQC NMR experiments SARS-CoV2 5'-end RNA structures with DMAs

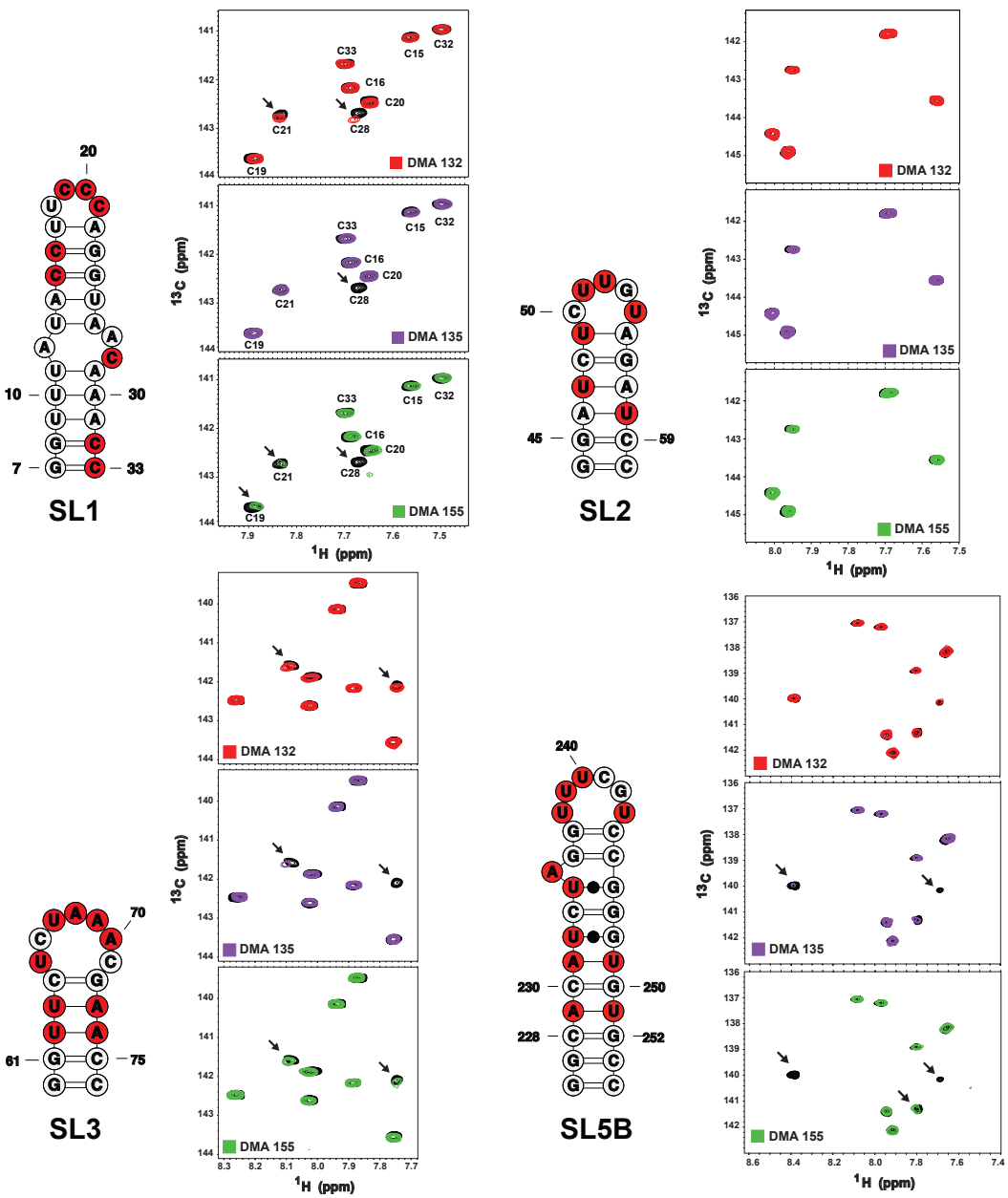

Figure S5. Single-point ^{13}C-^{1}H TROSY HSQC titrations of DMA-132 -135 and -155 with isolated SL domains of the SARS-CoV-2 5'-end.

VI. ^{1}H-^{1}H NOESY NMR experiments of selectively labeled SL1 with DMA-135 and SL6 with DMA-155

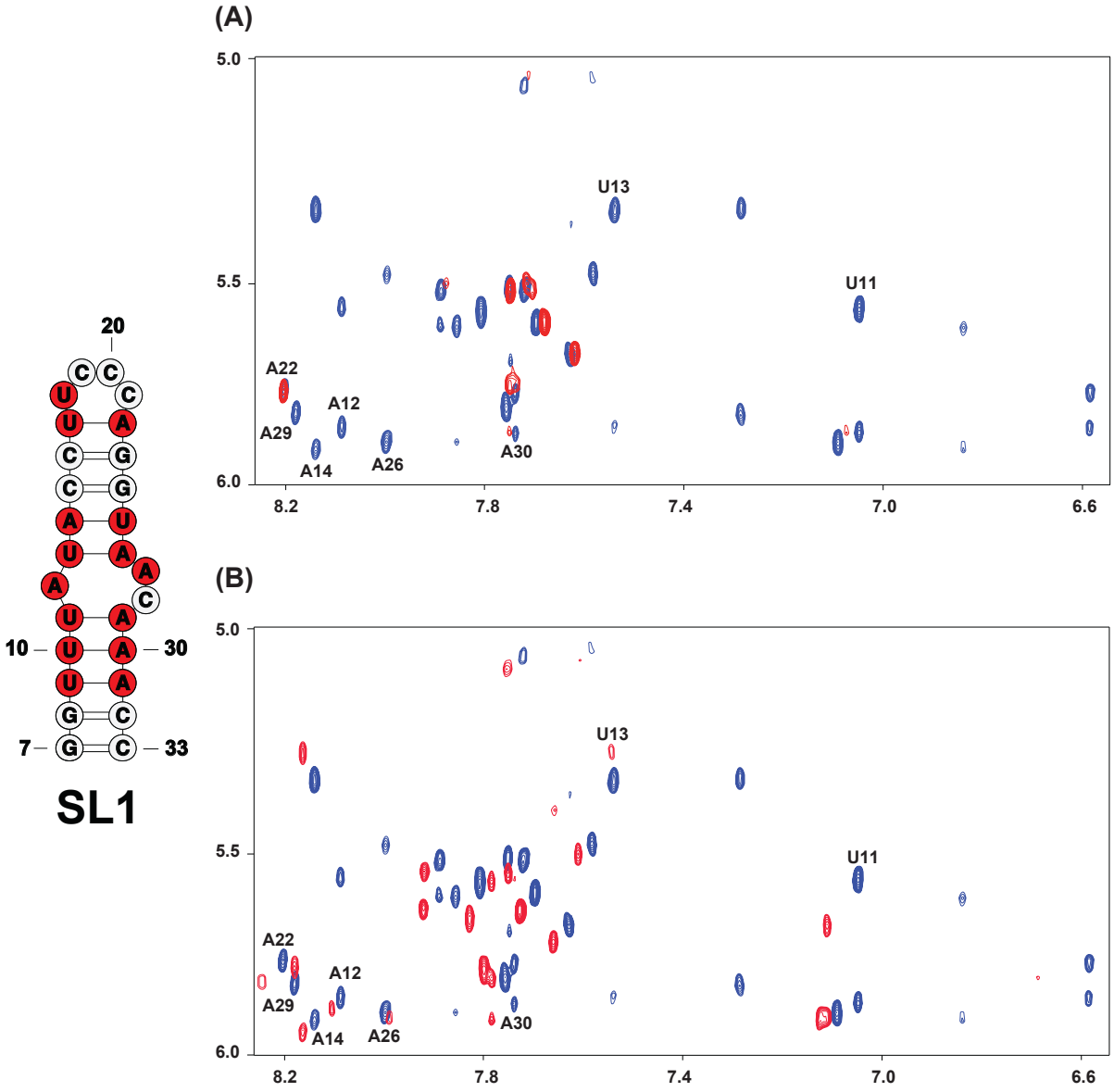

Figure S6. DMA-135 changes local structure of the SARS-Cov-2 5'-SL1 domain, while DMA-155 preserves it. (A) Overlay of ^{1}H-^{1}H NOESY spectra (t_m = 250 ms) of free GC(^{2}H), AU($^{2}H_{3',5''}$)-selectively labeled SL1 (blue) and the (DMA-135)-SL1 complex (red). **(B)** ^{1}H-^{1}H NOESY spectra overlay (t_m = 250 ms) of free GC(^{2}H), AU($^{2}H_{3',5''}$)-selectively labeled SL1 (blue) and the (DMA-155)-SL1 complex (red). All NMR spectra were collected at 900 MHz in 25 mM K2HPO4, 50 mM KCl, pH 6.2 D2O buffer at 303 K. The selectively labeled nucleotides are highlighted in red on the secondary structure of SL1.

VII. *In silico* screening of DMA focused library against 5'-end RNA structures

Table S1. Binding pockets identified with ICM pocket finder and characterization of each binding pocket.

SL	Volume	Area	Hydrophobicity	Buriedness	Aromatic	DLID	Radius	Nonsphericity
1.4	132.87	143.87	0.47	0.86	0.05	-0.63	3.17	1.14
1.2	111.15	211.04	0.26	0.56	0.00	-2.42	2.98	1.89
1.1	108.75	234.70	0.20	0.56	0.04	-2.59	2.96	2.13
3	111.58	124.56	0.52	0.85	0.00	-0.72	2.99	1.11
4.1	583.35	615.91	0.37	0.80	0.09	-0.02	5.18	1.82
4.2	142.86	192.83	0.35	0.68	0.02	-1.55	3.24	1.46
4.3	126.79	168.48	0.40	0.78	0.08	-1.15	3.12	1.38
5a.1	273.58	474.91	0.37	0.74	0.03	-0.81	4.03	2.33
5a.2	174.42	274.74	0.37	0.70	0.01	-1.29	3.47	1.82
5a.3	160.57	228.90	0.38	0.69	0.01	-1.37	3.37	1.60
5a.4	133.51	206.26	0.31	0.64	0.00	-1.86	3.17	1.63
5a.5	132.20	180.61	0.42	0.70	0.06	-1.39	3.16	1.44
5b	285.30	310.08	0.49	0.85	0.14	-0.04	4.08	1.48
6.2	235.09	215.04	0.61	0.95	0.11	0.45	3.83	1.17
6.1	219.49	239.54	0.57	0.76	0.20	-0.41	3.74	1.36

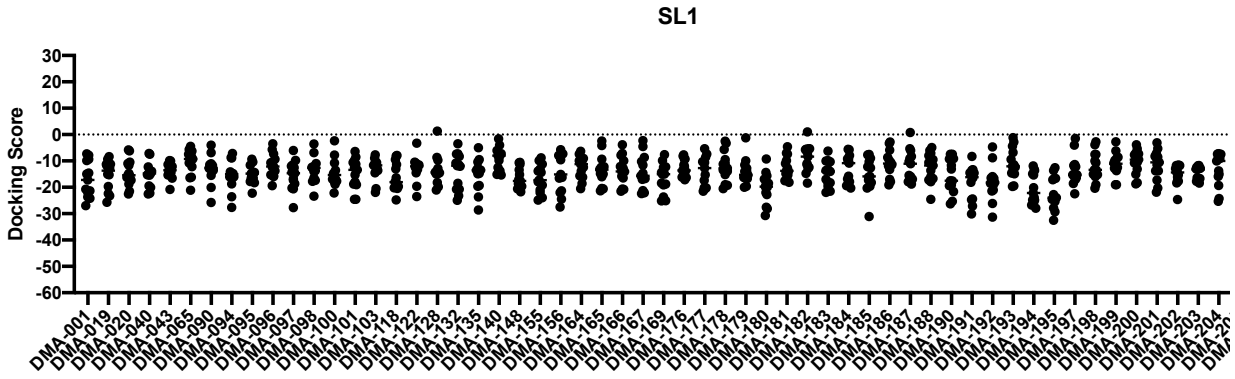

Figure S7. **Docking score of the 55 member DMA library against stem loop 1 (SL1).** The dots represent the best docking scores for each SL1 conformer present in the cluster of 10 structures.

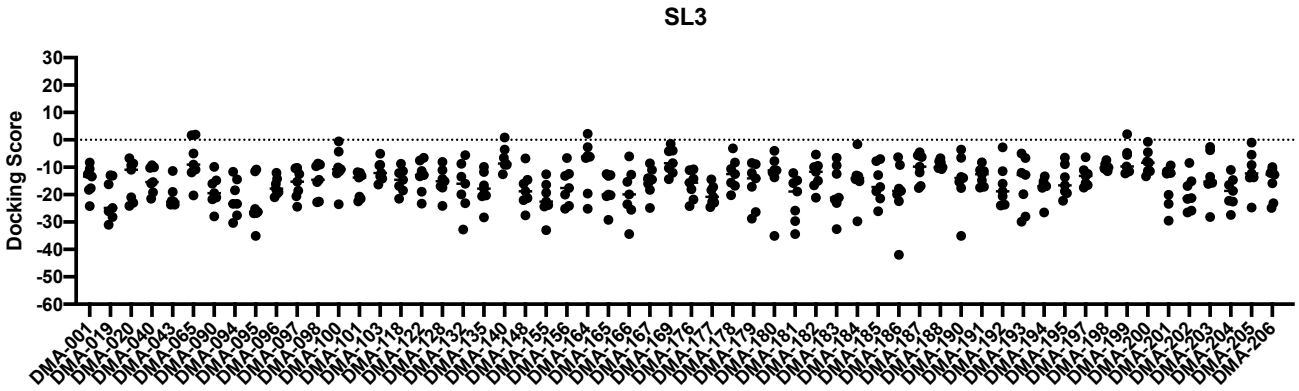

Figure S8. **Docking score of the 55 member DMA library against stem loop 3 (SL3).** The dots represent the best docking scores for each SL3 conformer present in the cluster.

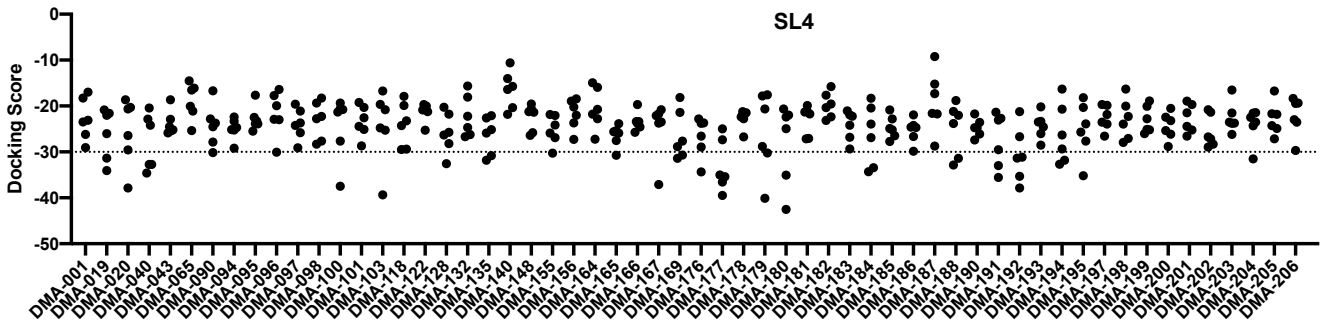

Figure S9. **Docking score of the 55 member DMA library against stem loop 4 (SL4)**. The dots represent the best docking scores for each SL4 conformer present in the cluster.

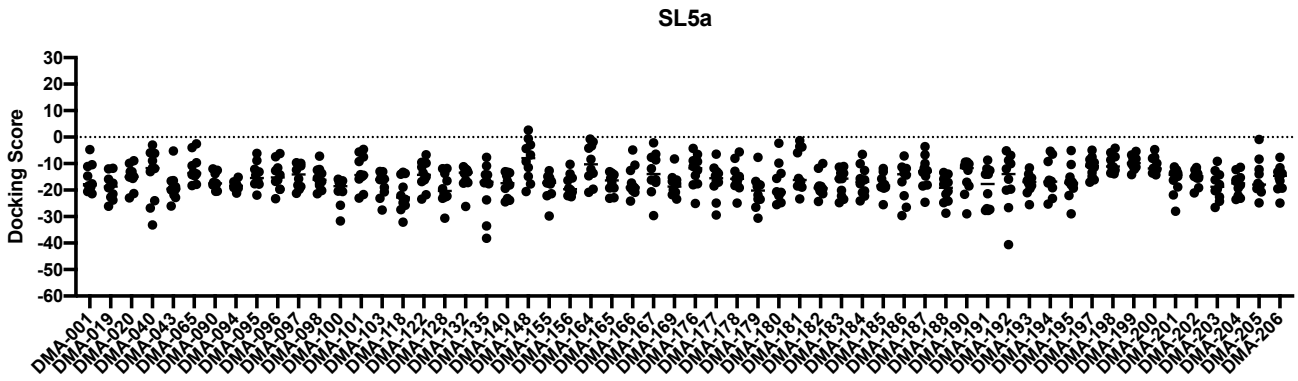

Figure S10. **Docking score of the 55 member DMA library against stem loop 5a (SL5a).** The dots represent the best docking scores for each SL5a conformer present in the cluster.

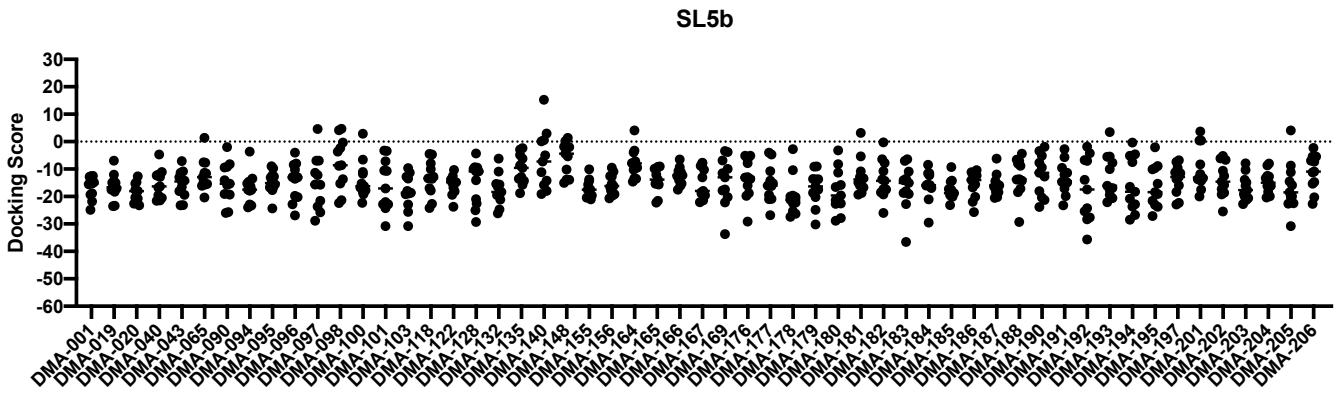

Figure S11. **Docking score of the 55 member DMA library against stem loop 5b (SL5b)**. The dots represent the best docking scores for each SL5b conformer present in the cluster.

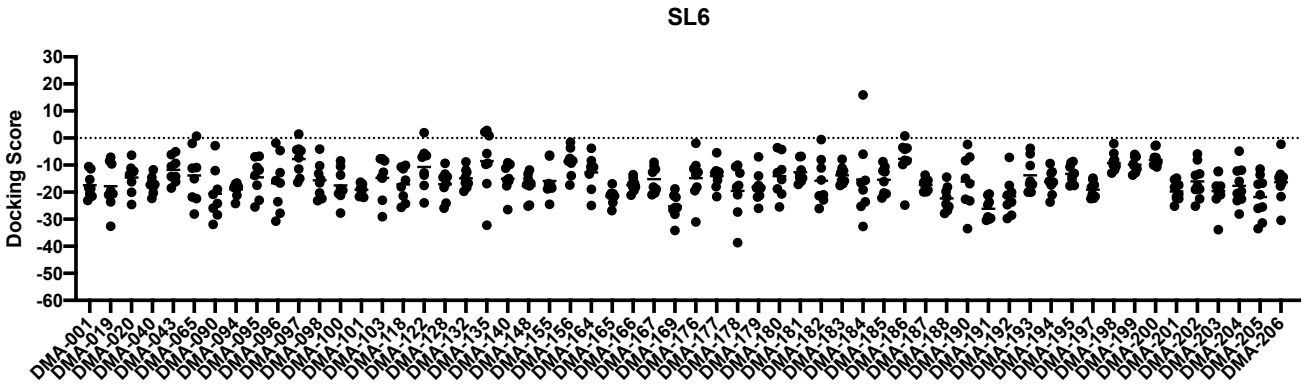

Figure S12. **Docking score of the 55 member DMA library against stem loop 6 (SL6)**. The dots represent the best docking scores for each SL6 conformer present in the cluster.

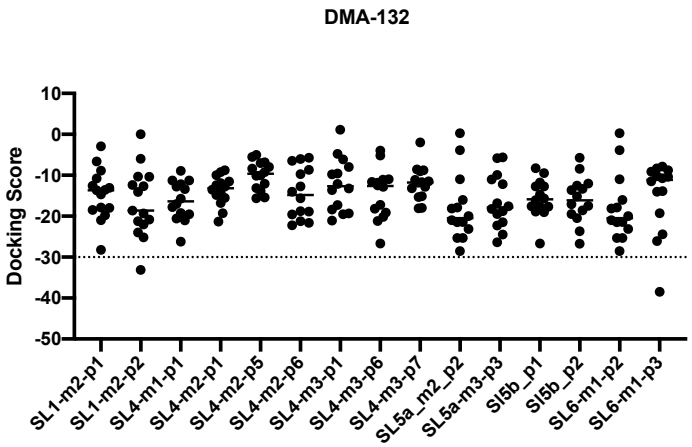

Figure S13. **Refined docking on motif-based clusters. Docking score of DMA-132 against every stem loop**. Columns represented correspond to pockets identified in bulge regions of motifs created around bulge or internal loop motifs. The dots correspond to the docking score of the molecule against each of the 15 conformers within the cluster.

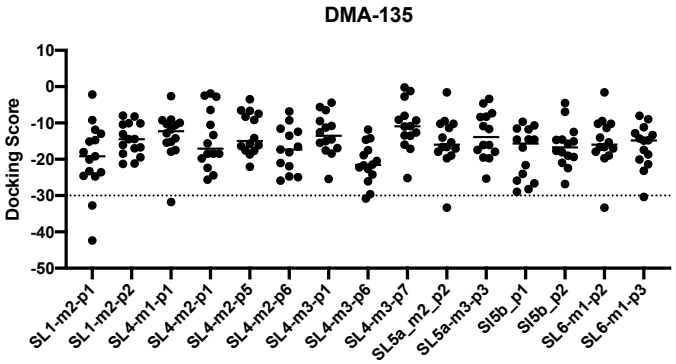

Figure S14. **Refined docking on motif-based clusters. Docking score of DMA-135 against every stem loop.** Columns represented correspond to pockets identified in bulge regions of motifs created around bulge or internal loop motifs. The dots correspond to the docking score of the molecule against each of the 15 conformers within the cluster.

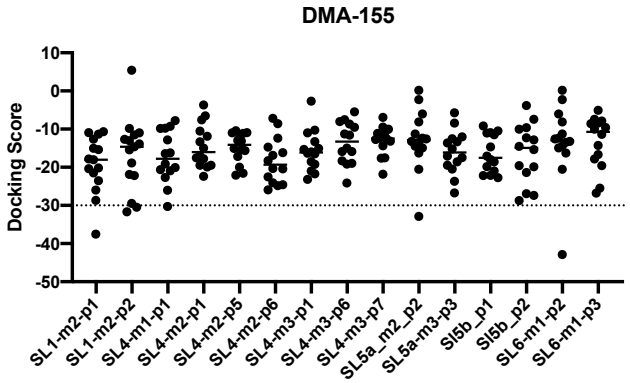

Figure S15. **Refined docking on motif-based clusters. Docking score of DMA-155 against every stem loop**. Columns represented correspond to pockets identified in bulge regions of motifs created around bulge or internal loop motifs. The dots correspond to the docking score of the molecule against each of the 15 conformers within the cluster.

VIII. *In vitro* fluorescence indicator displacement assay

A

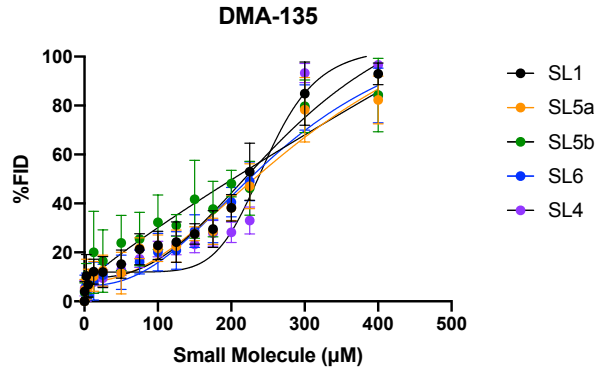

B

Stem Loop (SL)	Affinity (μM)
SL1	290.2 ± 6.6
SL4	248.1 ± 59.8
SL5a	333.0 ± 5.0
SL5b	$Out\ of\ range$
SL6	278.3 ± 4.0

Figure S16. **Indicator displacement assay (IDA) of DMA-135 against 5'-end stem loops.** (**A**) small molecule titration curve of DMA-135 with SL1, SL4, SL5a, SL5b, and SL6. Small molecule binding is plotted as a function % displacement and ligand concentration. (**B**) Affinity calculated for DMA-135 for each stem loop after three independent replicates.

A

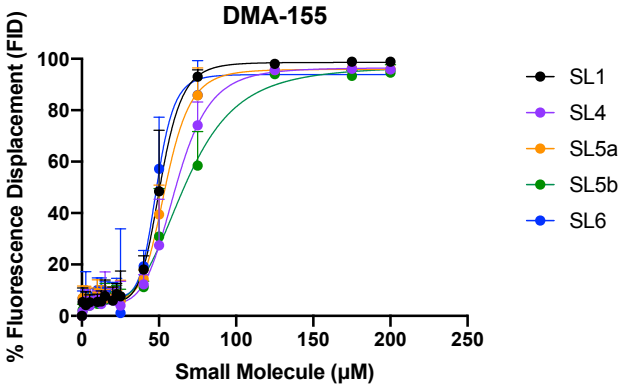

B

Stem Loop (SL)	Affinity (μM)
SL1	51.1 ± 1.9
SL4	61.1 ± 3.3
SL5a	54.5 ± 1.9
SL5b	66.9 ± 3.1
SL6	48.6 ± 1.6

Figure S17. **Indicator displacement assay (IDA) of DMA-135 against 5'-end stem loops.** (**A**) small molecule titration curve of DMA-155 with SL1, SL4, SL5a, SL5b, and SL6. Small molecule binding is plotted as a function % displacement and ligand concentration. (**B**) Affinity calculated for DMA-155 for each stem loop after three independent replicates